Efficient Multi-User MIMO Transmissions in the LTE-A Uplink

Lukas Nagel*, Stefan Pratschner*, Stefan Schwarz*†, and Markus Rupp*,
*Institute of Telecommunications, TU Wien, Austria
{lnagel,spratsch,sschwarz,mrupp}@nt.tuwien.ac.at
†Christian Doppler Laboratory for Dependable Wireless Connectivity for the Society in Motion

***Abstract*—Single-User Multiple-Input Multiple-Output (MIMO) transmissions are possible since Rel. 10 of 3GPP LTE-A. The Closed Loop Spatial Multiplexing (CLSM) transmission mode enables up to a four fold increase in spectral efficiency compared to Rel. 8, yet it requires complex User Equipment (UE) hardware supporting more than one transmit antenna. The closed loop spatial multiplexing transmission mode enables up to a four fold increase in spectral efficiency compared to Rel. 8, yet it requires complex UE hardware supporting more than one transmit antenna. As it is likely that the Base Station (BS) has more receive antennas than the UE transmit antennas, employing Multi-User (MU) MIMO transmissions in the uplink can lead to significant improvement in cell throughput. We formulate MU MIMO transmissions with linear receivers as a compact matrix system model. Based on our model we present a post-equalization SINR equation, allowing the calculation of a quantized feedback parameter, the Channel Quality Indicator (CQI) value. Within this framework we reveal possible MU gains through known scheduling algorithms although the frequency selective channel is approximated by its arithmetic mean.**

***Index Terms*—LTE-A, uplink, MU MIMO, MIMO MAC, scheduling.**

I. Introduction

Closed Loop Spatial Multiplexing (CLSM) based Single User Multiple-Input Multiple-Output (SU-MIMO), is supported since Rel. 10 of 3rd Generation Partnership Project (3GPP) UMTS Long Term Evolution-Advanced (LTE-A) in the uplink [1]. In this transmission mode, time-frequency resources are allocated exclusively to one user. A User Equipment (UE) then employs up to four spatial streams in uplink transmission, leading to an increase in peak spectral efficiency by a factor equal to the number of employed spatial streams. In order to exploit this spatial multiplexing gain, a UE needs more than a single transmit antenna and as many transmitter chains. This means very complex and power hungry UE hardware. Further, employing four transmit antennas on a small hand held device will likely result in antenna correlation, leading to a significant reduction in spatial multiplexing gain [2].

When multiple users have allocated the same resources and transmit simultaneously, their transmitted signals are separated in the spatial domain at the receiver side. This is commonly referred to as Multi-User (MU) Multiple-Input Multiple-Output (MIMO). The corresponding channel, as shown in Fig. 1, is known as Multiple Access Channel (MAC) [3], [4]. Although LTE-A allows for 4×4 MIMO in uplink transmissions since Rel. 10, it is likely that the number of receive antennas at the Base Station (BS) exceeds the number of transmit antennas of a UE. In such a scenario, the sum throughput is significantly increased when MU MIMO is employed [5], [6]. For this mode of operation, gains in sum throughput are achieved with linear receivers as well as with interference cancellation receivers [7]–[9]. When a linear receiver is employed, the number of single transmit antenna users should not exceed the number of receive antennas at the BS in order to resolve all received signals at the BS [10]. This implies a scheduling problem when more UEs than receive antennas are available in a cell [9], [11].

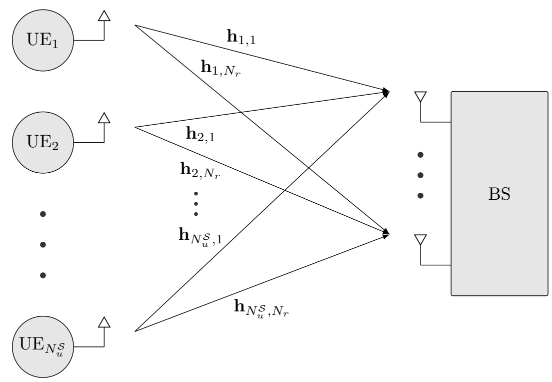

Fig. 1. Illustration of the MIMO MAC for LTE-A uplink.

For a UE with a single transmit antenna, link adaptation in LTE-A is performed by adapting the Modulation and Coding Scheme (MCS) to the current channel state. This is achieved by quantized Channel State Information (CSI) feedback from the BS to all scheduled UEs in terms of a Channel Quality Indicator (CQI) which is defined in [12].

We show sum rate improvements of MU MIMO transmissions over Single-User (SU) operation by means of simulation. Further we show that achieving MU gains in cell spectral efficiency is possible by employing known scheduling strategies even when the frequency selective channel's arithmetic mean is utilized. To show these effects we utilize the Vienna LTE-A Uplink Link Level Simulator [13]–[15]. Based on our introduced MU MIMO system model, we derive a post-equalization Signal to Interference and Noise Ratio (SINR) equation to enable the calculation of the CQI feedback parameter.

The paper is structured as follows. In Section II we introduce a transmission model in matrix notation which is exploited throughout the paper. We present a SINR equation and explain the link adaptation in Section III and introduce different scheduling strategies in Section IV. Simulation results and conclusions are given in Section V and Section VI, respectively.

II. System Model

Within our system, we assume that N_u UEs, with a single transmit antenna each, are attached to one BS. Out of all these N_u available users, the currently scheduled users u are combined in the schedule $\mathcal{S} \subseteq \{1, \ldots, N_u\}$, i.e., $u \in \mathcal{S}$. The number of scheduled users is then denoted by $N_u^{\mathcal{S}} = |\mathcal{S}|$.

The LTE-A uplink employs Single-carrier Frequency Division Multiplexing (SC-FDM) as physical layer access scheme. This is basically Discrete Fourier Transform (DFT) spreaded Orthogonal Frequency Division Multiplexing (OFDM), meaning that the transmit symbols are DFT spreaded at the transmitter side, and again de-spreaded by an Inverse Discrete Fourier Transform (IDFT) at the receiver side. We present our system model in a vector and matrix notation as in [14], [16].

The transmit symbols of scheduled user u for all N_{SC} subcarriers at OFDM symbol time n are described by vector $\mathbf{x}_{u,n} \in \mathbb{C}^{N_{\text{SC}} \times 1}$. These symbol vectors of all scheduled users with $u \in \mathcal{S}$ are then combined in vector $\mathbf{x}_n \in \mathbb{C}^{N_u^{\mathcal{S}} N_{\text{SC}} \times 1}$ as $\mathbf{x}_n = \left(\mathbf{x}_{1,n}^T, \ldots, \mathbf{x}_{N_u^{\mathcal{S}},n}^T\right)^T$. The transmit symbols are statistically independent and have transmit power $\sigma_{\mathbf{x}}^2$, i.e., $\mathbb{E}\{\mathbf{x}_n \mathbf{x}_n^H\} = \sigma_{\mathbf{x}}^2 \mathbf{I}_{N_u^{\mathcal{S}} N_{\text{SC}}}$. Further, channel coefficients of all subcarriers and all scheduled users are combined in the block-wise diagonal channel matrix $\mathbf{H} \in \mathbb{C}^{N_r N_{\text{SC}} \times N_u^{\mathcal{S}} N_{\text{SC}}}$ as

$$\mathbf{H} = \begin{pmatrix} \mathbf{H}_{1,1} & \mathbf{H}_{1,2} & \cdots & \mathbf{H}_{1,N_u^{\mathcal{S}}} \\ \mathbf{H}_{2,1} & \mathbf{H}_{2,2} & \cdots & \mathbf{H}_{2,N_u^{\mathcal{S}}} \\ \vdots & \vdots & \ddots & \vdots \\ \mathbf{H}_{N_r,1} & \mathbf{H}_{N_r,2} & \cdots & \mathbf{H}_{N_r,N_u^{\mathcal{S}}} \end{pmatrix} , \quad (1)$$

with diagonal matrices $\mathbf{H}_{r,u} \in \mathbb{C}^{N_{\text{SC}} \times N_{\text{SC}}}$, containing the channel coefficients from scheduled user $u \in \mathcal{S}$ to receive antenna $r \in \{1, \ldots, N_r\}$, i.e., $\mathbf{H}_{r,u} = \text{diag}(\mathbf{h}_{r,u})$. Assuming block fading, the channel is constant for the duration of a subframe, which equals 14 or 12 OFDM symbols for normal or extended Cyclic Prefix (CP) length, respectively. Further assuming the CP length to be sufficient, the vector of channel coefficients for all N_{SC} subcarriers from scheduled user u to receive antenna r, denoted by $\mathbf{h}_{r,u} \in \mathbb{C}^{N_{\text{SC}} \times 1}$, is obtained by the DFT of the zero padded vector of the time domain Channel Impulse Response (CIR) $\mathbf{h}'_{r,u} \in \mathbb{C}^{N_{\text{SC}} \times 1}$, i.e., $\mathbf{h}_{r,u} = \mathbf{D}_{N_{\text{SC}}} \mathbf{h}'_{r,u}$, where $\mathbf{D}_{N_{\text{SC}}}$ denotes a unitary DFT matrix of size $N_{\text{SC}} \times N_{\text{SC}}$.

As the LTE-A uplink employs SC-FDM, the transmit symbols $\mathbf{x}_n$ are DFT spreaded at each user prior to OFDM processing. At the receiver side, the de-spreading is of course carried out by an IDFT, again for each user. The estimated symbols at the receiver are therefore given by

$$\begin{aligned} \hat{\mathbf{x}}_n = & \underbrace{\left(\mathbf{I}_{N_u^{\mathcal{S}}} \otimes \mathbf{D}_{N_{\text{SC}}}^H\right) \mathbf{F}\mathbf{H} \left(\mathbf{I}_{N_u^{\mathcal{S}}} \otimes \mathbf{D}_{N_{\text{SC}}}\right)}_{\mathbf{K}} \mathbf{x}_n \\ & + \left(\mathbf{I}_{N_u^{\mathcal{S}}} \otimes \mathbf{D}_{N_{\text{SC}}}^H\right) \mathbf{F}\mathbf{z}_n \ , \end{aligned} \quad (2)$$

with the i.i.d. Gaussian noise vector $\mathbf{z}_n \sim \mathcal{CN}\left(0, \sigma_{\mathbf{z}}^2 \mathbf{I}_{N_u^{\mathcal{S}} N_{\text{SC}}}\right)$, the system matrix $\mathbf{K} \in \mathbb{C}^{N_u^{\mathcal{S}} N_{\text{SC}} \times N_u^{\mathcal{S}} N_{\text{SC}}}$ and the linear receiver $\mathbf{F} \in \mathbb{C}^{N_u^{\mathcal{S}} N_{\text{SC}} \times N_r N_{\text{SC}}}$.

For a Zero Forcing (ZF) receiver, the linear receiver $\mathbf{F}$ is obtained as

$$\mathbf{F}_{\text{ZF}} = \left(\mathbf{H}^H \mathbf{H}\right)^{-1} \mathbf{H}^H \ , \quad (3)$$

and in case of an Minimum Mean Square Error (MMSE) receiver it is given by

$$\mathbf{F}_{\text{MMSE}} = \left(\mathbf{H}^H \mathbf{H} + \sigma_{\mathbf{z}}^2 \mathbf{I}\right)^{-1} \mathbf{H}^H \ . \quad (4)$$

Due to the block-wise diagonal structure of $\mathbf{H}$, the receiver $\mathbf{F}$ is of the same structure. In the ZF case, i.e., $\mathbf{F}_{\text{ZF}}\mathbf{H} = \mathbf{I}$, inserting the linear receiver (3) into (2) leads to system matrix $\mathbf{K}_{\text{ZF}} = \mathbf{I}$, similar to the OFDM case. Due to the DFT de-spreading within the SC-FDM processing, this is different when an MMSE receiver is employed. Inserting (4) into (2), the product $\mathbf{F}_{\text{MMSE}}\mathbf{H}$ has a block-wise diagonal structure. The DFT and IDFT operations on this block-wise diagonal matrix in (2) finally yield a block-wise circulant system matrix $\mathbf{K}_{\text{MMSE}}$. In this case, the diagonal elements of $\mathbf{K}$ represent the desired signal while all other elements describe interference. This means, that in an SC-FDM system, not only inter-user interference but also inter-sample interference occurs when an MMSE receiver is employed. Still, since the post-equalization SINR in SC-FDM is dominated by the worst subcarrier when a ZF receiver is employed [14], utilizing an MMSE receiver leads to better performance in terms of throughput as we show in Section V.

The block-wise diagonal structures of $\mathbf{H}$ and $\mathbf{F}$ allow for efficient calculation of the matrix inverse in (3) and (4). Due to the matrix structure, only the non zero matrix elements on the block-diagonals have to be considered which leads to a inverse calculation on subcarrier basis. This means, instead of inverting a $N_u^{\mathcal{S}} N_{\text{SC}} \times N_u^{\mathcal{S}} N_{\text{SC}}$ matrix directly, N_{SC} matrices of size $N_u^{\mathcal{S}} \times N_u^{\mathcal{S}}$ are inverted.

III. Link Adaptation

Since we assume UEs with a single transmit antenna, each user is transmitting on a single spatial layer. In this case link adaptation in LTE-A uplink is carried out by adjusting the MCS to the current channel condition. For this, quantized feedback of the current CSI is signalled from the BS to the UE in terms of a CQI value. This value is calculated at the receiver side, utilizing the post-equalization SINR [17]. By employing a mapping function obtained by simulations on a Single-Input Single-Output (SISO) Additive White Gaussian Noise (AWGN) channel, the post equalization SINR is mapped to a CQI value such that the a target Block Error Ratio (BLER) of 0.1 is reached [18].

Exploiting the system matrix $\mathbf{K}$ as defined in (2) the post-equalization SINR of user u after de-spreading is given by

$$\mathrm{SINR}_u = \frac{\sigma_{\mathbf{x}}^2 \left\|\mathbf{S}_u \mathrm{diag}(\mathbf{K})\right\|_F^2}{\sigma_{\mathbf{x}}^2 \left\|\mathbf{S}_u \mathbf{K}\right\|_F^2 - \sigma_{\mathbf{x}}^2 \left\|\mathbf{S}_u \mathrm{diag}(\mathbf{K})\right\|_F^2 + \sigma_{\mathbf{z}}^2 \left\|\mathbf{D}^H \mathbf{S}_u \mathbf{F}\right\|_F^2} , \quad (5)$$

with selection matrix $\mathbf{S}_u \in \{0,1\}^{N_{\mathrm{SC}} \times N_u^{\mathcal{S}} N_{\mathrm{SC}}}$ given by

$$\mathbf{S}_u = \big(\underbrace{\mathbf{0}_{N_{\mathrm{SC}}}, \ldots, \mathbf{0}_{N_{\mathrm{SC}}}}_{\substack{u-1 \\ \text{zero matrices}}}, \mathbf{I}_{N_{\mathrm{SC}}}, \mathbf{0}_{N_{\mathrm{SC}}}, \ldots, \mathbf{0}_{N_{\mathrm{SC}}}\big) . \quad (6)$$

As already explained in Section II, the diagonal of $\mathbf{K}$ describes the desired signal, while all other elements describe interference. This is exploited in (5) where all elements, but the ones on the diagonal, of $\mathbf{K}$ contribute to the interference power.

Since the DFT spreading and de-spreading in (2) leads to a block-wise circulant system matrix $\mathbf{K}$, the post equalization SINR is the same for all subcarriers k as already shown in [19]. Calculating the SINR for a single subcarrier is therefore equivalent to averaging the SINR over all subcarriers, which is expressed by the Frobenius norm in (5). A CQI value for user u is then obtained by exploiting the post-equalization SINR in an SINR to CQI mapping, including quantization, which is described by the function

$$\mathrm{CQI}_u = f\left(\mathrm{SINR}_u\right) , \quad (7)$$

and further explained in [17], [18].

IV. Scheduling

Exploiting a linear receiver, the number of scheduled users $N_u^{\mathcal{S}}$ must not exceed the number of receive antennas N_r in order to resolve all received signals at the BS. We therefore distinguish whether the total number of users N_u is smaller or equal to N_r, or the number of users is higher than the antenna count. In the first case we employ the simplest scheduling strategy which is to schedule all UEs. In the second case the BS has to decide which UEs are scheduled in a specific subframe. In the following we discuss this latter case.

In general the selection of the $N_u^{\mathcal{S}}$ UEs to schedule demands a trade-off between maximising the collaborative sum throughput and ensuring fairness between the users as done in [11], [20]. However, in our work we do not take fairness into consideraton but focus on scheduling strategies aiming for sum throughput maximization.

LTE-A allows scheduling on a ressource block basis. It is therefore possible to schedule more UEs at different frequencies and to change the schedule twice per subframe. Due to the blockfading assumption we determine a schedule only once per subframe and furthermore assign all frequencies to one user to reduce complexity. Finding the subset of UEs that leads to maximum cell throughput, assuming that N_r UEs are scheduled, is still a computationally demanding task, as the number of possible schedules is given by $\binom{N_u}{N_r}$. An exhaustive search over all those combinations is not feasible in real time processing [11]. It is therefore necessary to find more efficient ways for user selection.

One way to calculate the schedule is according to the Semi-orthogonal User Selection (SUS) algorithm proposed by [21]. To apply the algorithm we first consider $\tilde{\mathbf{H}} \in \mathbb{C}^{N_r N_{\mathrm{SC}} \times N_u N_{\mathrm{SC}}}$ which shares its structure with the block-wise diagonal channel matrix $\mathbf{H}$ from (1) but contains the channels of all N_u UEs. We first extract the channel of one sub-carrier

$$\mathbf{H}_k = \begin{pmatrix} \mathrm{diag}\left(\tilde{\mathbf{H}}_{1,1}\right)_k & \cdots & \mathrm{diag}\left(\tilde{\mathbf{H}}_{1,N_u}\right)_k \\ \vdots & \ddots & \vdots \\ \mathrm{diag}\left(\tilde{\mathbf{H}}_{N_r,1}\right)_k & \cdots & \mathrm{diag}\left(\tilde{\mathbf{H}}_{N_r,N_u}\right)_k \end{pmatrix} , \quad (8)$$

where $\mathrm{diag}\left(\mathbf{H}_{i,j}\right)_k$ selects the k-th element in the diagonal of $\mathbf{H}_{i,j}$, resulting in a subcarrier wise channel matrix $\mathbf{H}_k \in \mathbb{C}^{N_r \times N_u}$. For a scheduling algorithm however, a representation of the whole channel for all subcarriers is necessary. We assume the subcarriers of the frequency selective channel to be strongly correlated and replace the channel matrix $\mathbf{H}_k$ by its linear Taylor approximation around its arithmetic mean as in [22]. This yields

$$\bar{\mathbf{H}} = \frac{1}{N_{\mathrm{SC}}} \sum_{k=1}^{N_{\mathrm{SC}}} \mathbf{H}_k = \left(\bar{\mathbf{h}}_1, \bar{\mathbf{h}}_2, \cdots \bar{\mathbf{h}}_{N_u}\right) , \quad (9)$$

which describes the channel from all N_u UEs to the N_r receive antennas. The columns $\bar{\mathbf{h}}_i$ of $\bar{\mathbf{H}}$ are an average of the channel coefficients from one UE to all receive antennas.

The goal of the SUS algorithm is to find a set of UEs such that their corresponding channel coefficient vectors $\bar{\mathbf{h}}_i$ are (close to) orthogonal to each other to minimise their interference. In the following we describe the implementation in more detail.

For the initialisation we define an empty set of indices $\mathcal{S}$ which the algorithm fills with the indices of the scheduled users, set the matrix $\mathbf{T}_1 = \bar{\mathbf{H}}$ that includes channel coefficients that may be scheduled, set the loop index $i = 1$ and then execute these steps repeatedly:

1) Calculate the projection matrix

$$\mathbf{P}_i = \left(\mathbf{I} - \sum_{j=1}^{i-1} \frac{\mathbf{g}_j \mathbf{g}_j^H}{\left\|\mathbf{g}_j\right\|^2}\right) , \quad (10)$$

which is $\mathbf{I}$ in the first iteration.

2) Exploit the matrix $\mathbf{P}_i$ to remove the channel vectors components $\bar{\mathbf{h}}_k$ in $\mathbf{T}_i \in \mathbb{C}^{N_r \times t_i}$ into the direction of the previously selected vectors $\mathbf{g}_j$ to obtain

$$\tilde{\mathbf{G}}_i = \mathbf{P}_i \mathbf{T}_i = \left(\bar{\mathbf{g}}_1, \bar{\mathbf{g}}_2, \ldots, \bar{\mathbf{g}}_{t_i}\right) , \quad (11)$$

which contains the part of vectors in $\mathbf{T}_i$ that are orthogonal to $\mathbf{g}_j$ as column vectors.

3) Now select the i-th user by

$$k_{\max} = \underset{k \in \{1,\ldots,t_i\}}{\arg\max} \|\bar{\mathbf{g}}_k\|, \quad \mathcal{S} \leftarrow \mathcal{S} \cup \{k_{\max}\} , \quad (12)$$

as the user that has the biggest norm $\|\bar{\mathbf{g}}_k\|$ and add it to the selected users set $\mathcal{S}$.

4) If $|\mathcal{S}| = N_r$ the algorithm stops and all users with an index $k \in \mathcal{S}$ are scheduled. Otherwise we set the new

$$\mathbf{T}_{i+1} \leftarrow \bar{\mathbf{h}}_k : \frac{\bar{\mathbf{h}}_k^H \mathbf{g}_{k_{\max}}}{\|\bar{\mathbf{h}}_k\| \|\mathbf{g}_{k_{\max}}\|} < \alpha, \ k \in \{1, \ldots, t_i\} \backslash k_{\max} \quad (13)$$

combining all remaining columns of $\mathbf{T}_i$ that are close to orthogonal to the new $\mathbf{g}_{k_{\max}}$. In this equation $\alpha \in (0, 1)$ is a parameter that determines if the other vectors need to be almost orthogonal to $\mathbf{g}_{k_{\max}}$ ($\alpha \approx 0$) or not ($\alpha \to 1$). If $\mathbf{T}_{i+1}$ is empty the algorithm terminates and all users in $\mathcal{S}$ are scheduled. Otherwise, add the selected vector $\mathbf{g}_{k_{\max}}$ to previously selected vectors $\mathbf{g}_j$ into the matrix $\mathbf{G} = (\mathbf{g}_1, \ldots, \mathbf{g}_{i-1})$ by

$$\mathbf{G} \leftarrow (\mathbf{G}, \mathbf{g}_{k_{\max}}) \ , \quad (14)$$

and increment the loop index $i \leftarrow i + 1$.

Adding users to schedule $\mathcal{S}$ based on criterion (13) does not necessarily lead to an increase in sum spectral efficiency. A performance gain for this algorithm is therefore achieved when a user is only added to the schedule if the sum spectral efficiency is actually increased, as done in Sec. III.C of [23].

Changing the parameter α leads to a trade-off between an on average faster algorithm for small values of α because less vectors are selected in (13) and one with more iterations but closer to orthogonal channel coefficient vectors for α close to 1. We found that due to the application of the arithmetic mean in (9) the overall throughput is not sensitive to a variation of α.

V. Simulation Results

All simulations were done with the Vienna LTE-A Uplink Link Level Simulator [13]–[15] applying TU channel model [24] and simulation parameters given as in Table I. In our simulations we consider a single BS with N_u attached UEs and compare the combined sum throughput of all the users. We assume perfect channel knowledge of all user channels at the BS and a block-fading channel as mentioned in the introduction.

TABLE I
Simulation Parameters

Parameter	Value
System Bandwidth	1.4 MHz
Number of Subcarriers N_{SC}	72
Feedback Delay	0 TTI
Antenna Configurations	1×4 SIMO
	4×4 SU-MIMO
	1×4 MU-MIMO
Receiver	ZF/MMSE
Channel Model	Typical Urban (TU) [24]
Channel Estimation	perfect channel knowledge

To compare different transmission and MIMO modes we assume a BS with four receive antennas and $N_u = 4$ attached users. Simulation results of this comparison are shown in Fig. 2. In the *SIMO* case, all four UEs have a single transmit antenna and are Round Robin scheduled on subframe basis, as explained in Section IV. Obviously the spectral efficiency is limited as only one spatial stream is employed. For *SU-MIMO*, each user has four transmit antennas and transmits in the closed loop spatial multiplexing mode employing a rank adaptive transmission [17] with up to four spatial streams. The cell throughput therefore saturates at four times the throughput of the *SIMO* case. When *MU-MIMO* is employed, each user is again equipped with a single transmit antenna. In this mode however, the MMSE receiver (4) is employed and since the number of receive antennas equals the number of users, all UEs are scheduled on all resources. This is not an optimal scheduling strategy but is done for comparability of results. It is clearly visible that *MU-MIMO* outperforms *SU-MIMO* by approximately 2 dB.

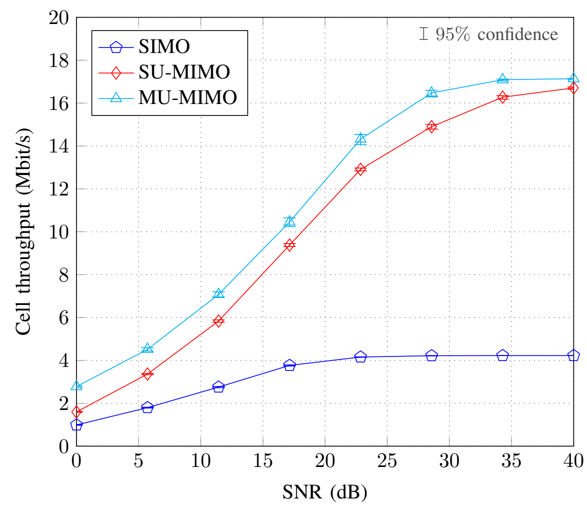

Fig. 2. Cell throughput comparison with $N_u = 4$ users employing 1x4 SIMO, 4x4 SU-MIMO with round robin and MU-MIMO with an MMSE receiver.

In Section II we proposed the ZF receiver (3) and the MMSE receiver (4) as two options for our linear receiver. While the ZF receiver cancels all the interference at the cost of, especially in low Signal to Noise Ratio (SNR) regime, considerable noise enhancement, the MMSE receiver instead attempts to minimize the overall error. As already explained, this leads to inter-user and inter-symbol interference in an SC-FDM system. Still, MMSE should always be preferred over the ZF receiver as shown in Fig. 3.

If there are more single transmit antenna UEs than receive antennas and a linear receiver is employed, the BS has to decide which users to schedule. In Fig. 4 we simulated a total number of $N_u = 10$ UEs with a single transmit antenna each, and a BS that is equipped with $N_r = 4$ receive antennas. First we show the *Random scheduler* curve where $N_u^{\mathcal{S}} = N_r = 4$ users are picked randomly. This performs the same as the *MUMIMO* case in Fig. 2 which was for $N_r = N_u = 4$ because the MU gain is not exploited. The upper bound on the MU gain is found by *Exhaustive search* over all possible schedules to maximize the sum throughput. Its gain over the *Random scheduler* throughput is the achievable scheduling gain of approximately 5 dB. As a low complexity alternative to

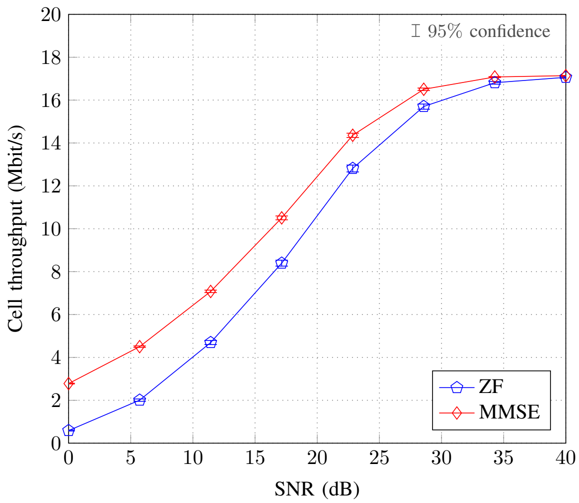

Fig. 3. Cell throughput comparison with $N_u = 4$ users for ZF and MMSE receivers.

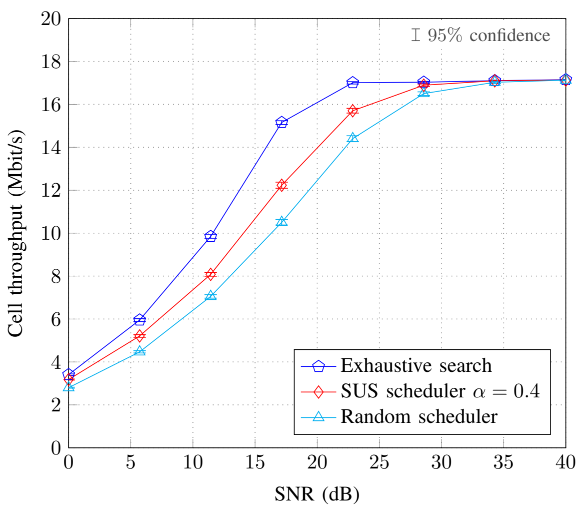

Fig. 4. Cell throughput for scheduling with exhaustive search, the SUS algorithm and randomly selecting users with MMSE receiver.

Exhaustive search we also show the performance of the *SUS scheduler* from Section IV. Although the complexity is low and the arithmetic average of the frequency selective schedule was considered within the algorithm, the achieved scheduling gain is in the order of 2 dB for $N_u = 10$ available users. However, the performance of the *SUS scheduler* theoretically approaches the *Exhaustive search* performance for $N_u \to \infty$.

VI. Conclusion

Exploiting the MU MIMO system model from Section II, we presented a post-equalization SINR equation that is utilized for feedback parameter calculation. Exploiting this link adaptation together with linear receivers, we showed significant gains in cell spectral efficiency by simulations, especially for an MMSE receiver. Further, we showed that potential MU gains through scheduling are significant, even when the arithmetic average of a frequency selective channel is considered for the user pairing algorithm.

Acknowledgements

This work has been funded by A1 Telekom Austria AG and the Institute of Telecommunications, TU Wien. The financial support by the Austrian Federal Ministry of Science, Research and Economy and the National Foundation for Research, Technology and Development is gratefully acknowledged.

References

[1] 3rd Generation Partnership Project (3GPP), "Evolved Universal Terrestrial Radio Access (E-UTRA) physical channels and modulation," 3rd Generation Partnership Project (3GPP), TS 36.211, Jan. 2015.

[2] H. Shin and J. H. Lee, "Capacity of multiple-antenna fading channels: spatial fading correlation, double scattering, and keyhole," *IEEE Transactions on Information Theory*, vol. 49, no. 10, pp. 2636–2647, 2003.

[3] D. N. C. Tse, P. Viswanath, and L. Zheng, "Diversity-Multiplexing Tradeoff in Multiple-Access Channels," *IEEE Transactions on Information Theory*, vol. 50, no. 9, pp. 1859–1874, Sep. 2004.

[4] M. Kobayashi and G. Caire, "Iterative Waterfilling for Weighted Rate Sum Maximization in MIMO-MAC," in *IEEE 7th Workshop on Signal Processing Advances in Wireless Communications (SPAWC'06)*, Jul. 2006, pp. 1–5.

[5] R. Ratasuk and A. Ghosh, "System performance of uplink multi-user MIMO in LTE," in *IEEE Vehicular Technology Conference (VTC Fall)*, 2011, pp. 1–5.

[6] Y. Yan, H. Yuan, N. Zheng, and S. Peter, "Performance of uplink multi-user MIMO in LTE-advanced networks," in *IEEE International Symposium on Wireless Communication Systems (ISWCS)*, 2012, pp. 726–730.

[7] X. Lv, T. Zhang, Z. Zeng, and L. Wang, "Uplink multi-user MIMO interference cancellation algorithm for LTE-A systems," in *IEEE International Conference on Information Networking and Automation (ICINA)*, vol. 1, 2010, pp. V1–294.

[8] B. Sah, M. Surendar, and P. Muthuchidambaranathan, "A frequency domain joint MMSE-SIC equalizer for MIMO SC-FDMA LTE-A uplink," in *IEEE International Conference on Electronics and Communication Systems (ICECS)*, 2014, pp. 1–4.

[9] L. Mroueh, E. Vivier, F. Z. Kaddour, M. Pischella, and P. Martins, "Combined ZF and ML decoder for uplink scheduling in multi-user MIMO LTE networks," in *IEEE 24th International Symposium on Personal Indoor and Mobile Radio Communications (PIMRC)*, 2013, pp. 1255–1259.

[10] D. Tse and P. Viswanath, *Fundamentals of wireless communication*. Cambridge university press, 2005.

[11] L.-H. Hsu, H.-L. Chao, C.-L. Liu, and K.-L. Huang, "Multi-user MIMO scheduling in LTE-Advanced uplink systems," in *IEEE 24th International Symposium on Personal Indoor and Mobile Radio Communications (PIMRC)*, 2013, pp. 1811–1816.

[12] 3rd Generation Partnership Project (3GPP), "Evolved Universal Terrestrial Radio Access (E-UTRA); Physical layer procedures," 3rd Generation Partnership Project (3GPP), TS 36.213, Jan. 2015.

[13] J. Blumenstein, J. C. Ikuno, J. Prokopec, and M. Rupp, "Simulating the Long Term Evolution Uplink Physical Layer," in *Proc. of the 53rd International Symposium ELMAR-2011*, Zadar, Croatia, Sept. 2011.

[14] E. Zöchmann, S. Schwarz, S. Pratschner, L. Nagel, M. Lerch, and M. Rupp, "Exploring the physical layer frontiers of cellular uplink," *EURASIP Journal on Wireless Communications and Networking*, 2016.

[15] [Online]. Available: http://www.nt.tuwien.ac.at/ltesimulator/

[16] A. Wilzeck, Q. Cai, M. Schiewer, and T. Kaiser, "Effect of Multiple Carrier Frequency Offsets in MIMO SC-FDMA Systems," in *Proceedings of the International ITG/IEEE Workshop on Smart Antennas*, 2007.

[17] S. Schwarz and M. Rupp, "Throughput maximizing feedback for MIMO OFDM based wireless communication systems," in *IEEE International Workshop on Signal Processing Advances in Wireless Communications (SPAWC)*, San Francisco, CA, USA, June 2011, pp. 316–320.

[18] J. C. Ikuno, M. Wrulich, and M. Rupp, "System level simulation of LTE networks," in *IEEE Vehicular Technology Conference (VTC Spring)*, Taipei, Taiwan, May 2010.

[19] E. Zöchmann, S. Pratschner, S. Schwarz, and M. Rupp, "MIMO transmission over high delay spread channels with reduced cyclic prefix length," in *Proc. of Workshop on Smart Antennas (WSA'15)*, Ilmenau, Germany, Feb. 2015.

[20] Z. Li, Y. Du, and C. Feng, "An uplink user selection scheme based on PF criterion for multi-user MIMO systems in LTE-A," in *IET International Conference on Communication Technology and Application (ICCTA 2011)*, 2011, pp. 121–125.

[21] T. Yoo and A. Goldsmith, "On the optimality of multiantenna broadcast scheduling using zero-forcing beamforming," *IEEE Journal on Selected Areas in Communications*, vol. 24, no. 3, pp. 528–541, 2006.

[22] S. Schwarz, M. Wrulich, and M. Rupp, "Mutual information based calculation of the precoding matrix indicator for 3GPP UMTS/LTE," in *2010 International ITG Workshop on Smart Antennas (WSA)*. IEEE, 2010, pp. 52–58.

[23] S. Schwarz and M. Rupp, "Evaluation of distributed downlink multi-user MIMO-OFDM with limited feedback," *IEEE Transactions on Wireless Communications*, vol. 13, pp. 6081–6094, Nov. 2014. [Online]. Available: http://ieeexplore.ieee.org/stamp/stamp.jsp?arnumber=6873345

[24] 3rd Generation Partnership Project (3GPP), "Universal Mobile Telecommunications System (UMTS) Deployment aspects," 3rd Generation Partnership Project (3GPP), TR 25.943, Feb. 2010.